

Figure S1. Energy dispersive X-ray spectroscopy (EDX) of pristine HfO_2 and selected $\text{Hf}_{1-x}\text{Ce}_x\text{O}_2$ nanocrystals. The detected concentrations of hafnium and cerium are listed in Table S1.

| Precursor Hf Concentration (Relative at.%) | Detected Hf Concentration by EDX (Relative at. %) | Detected Ce Concentration by EDX (Relative at. %) |
|--|---|---|
| 100 | 100 | 0 |
| 80 | 100 | Not Detected |
| 60 | 99.75 | 0.25 |
| 50 | 96.13 | 3.87 |

Table S1. Detected concentrations of hafnium and cerium by EDX analysis based on integration of the data shown in Figure S1.

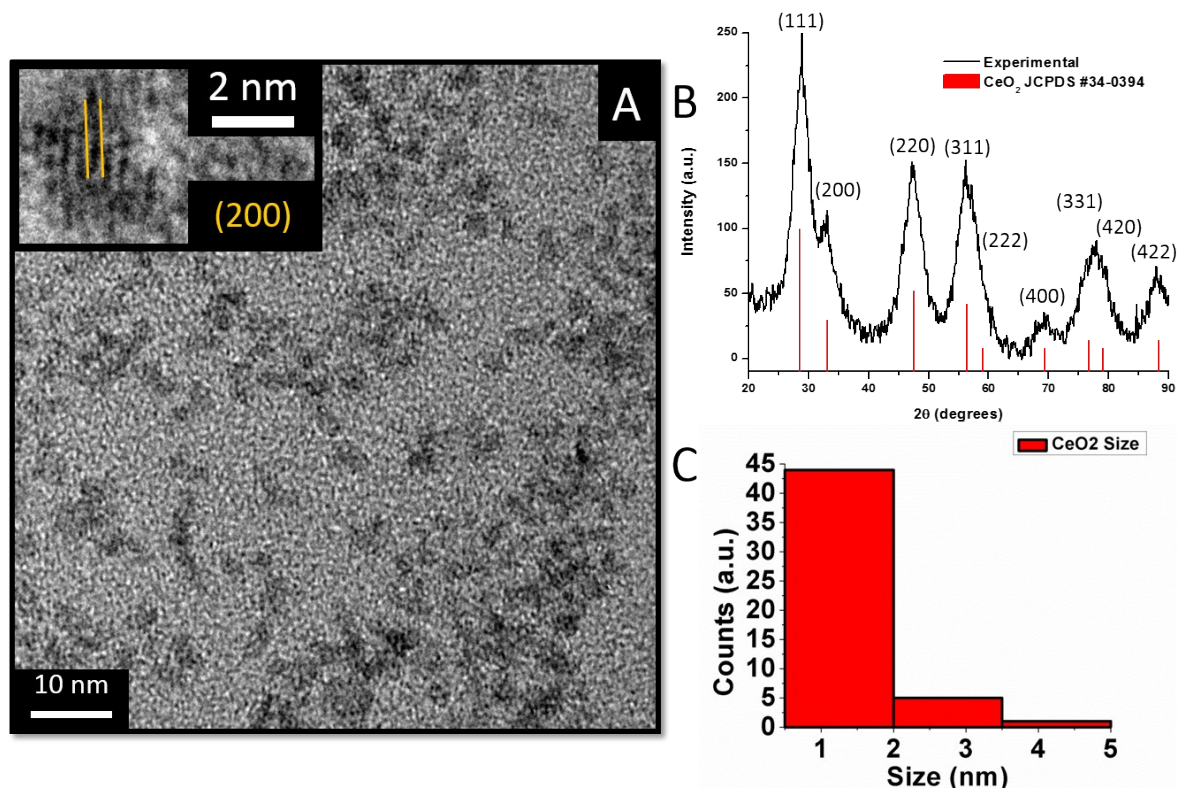


Figure S2. (A) Low-magnification transmission electron microscopy image of CeO₂ nanocrystals. The inset shows a HRTEM image indicating the separation between the (200) lattice planes of the cubic phase. (B) X-ray diffraction pattern of CeO₂ nanocrystals synthesized using 2 mmol of CeCl₃ and 2 mmol of Ce(OⁱBu)₄. Reflections of cubic CeO₂ are indicated in red (JCPDS # 34-0394). (C) Size distribution histogram indicating the size of the CeO₂ nanoparticles to be ca. 1.5 ± 0.5 nm.

| HfO ₂ (Monoclinic) – JCPDS # 78-0050 | | | | |
|--|------------|------------|------------|-----------|
| atom | x | y | z | occupancy |
| Hf1 | 0.2755(2) | 0.0397(1) | 0.2080(2) | 1.0 |
| O1 | 0.0739(20) | 0.3318(17) | 0.3466(17) | 1.0 |
| O2 | 0.4489(20) | 0.7582(16) | 0.4800(22) | 1.0 |
| Space Group = $P2_1/c$, $a = 5.1170(1)$, $b = 5.1754(2)$, $c = 5.2915(2)$ $\alpha, \gamma = 90$, $\beta = 99.216(2)$ | | | | |
| HfO ₂ (Tetragonal) – From Ref. 40 | | | | |
| atom | x | y | Z | occupancy |
| Hf1 | 0.0 | 0.0 | 0.0 | 1.0 |
| Hf2 | 0.5 | 0.5 | 0.5 | 1.0 |
| O1 | 0.5 | 0.0 | 0.21282 | 1.0 |
| O2 | 0.5 | 0.0 | -0.28718 | 1.0 |
| O3 | 0.0 | 0.5 | 0.28718 | 1.0 |
| O4 | 0.0 | 0.5 | -0.21282 | 1.0 |
| Space Group = $P4_2/nmc$, $a, b = 3.560000$, $c = 5.110000$, $\alpha, \beta, \gamma = 90$ | | | | |

Table S2. Unit cell parameters for the monoclinic and tetragonal phases of HfO₂.

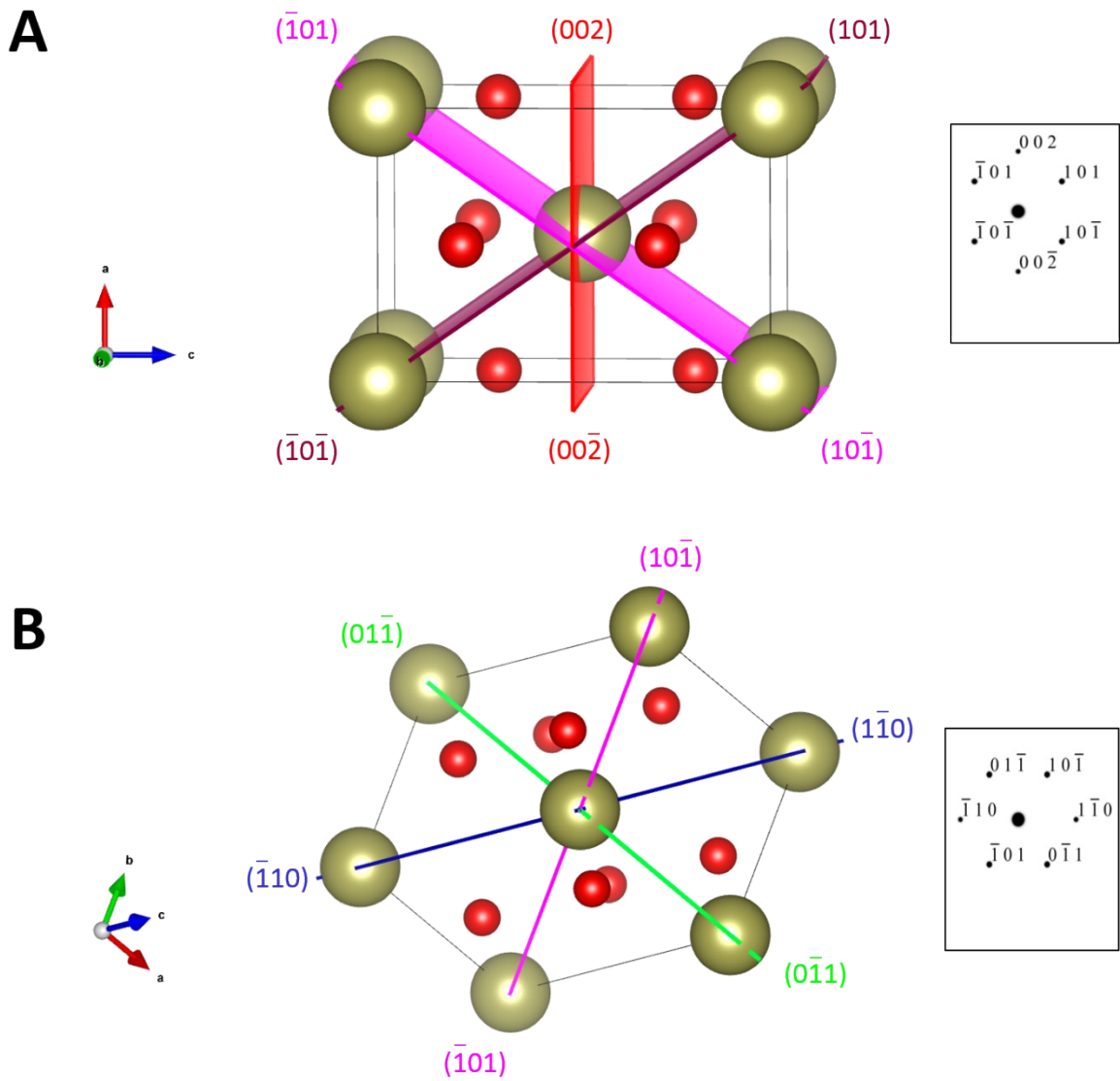


Figure S3. (A) HfO_2 tetragonal unit cell depicting the corresponding lattice planes from Figure 3D. (B) HfO_2 tetragonal unit cell depicting the corresponding lattice planes from Figure 3H. The unit cells were constructed using the lattice parameters given in Ref. 40.

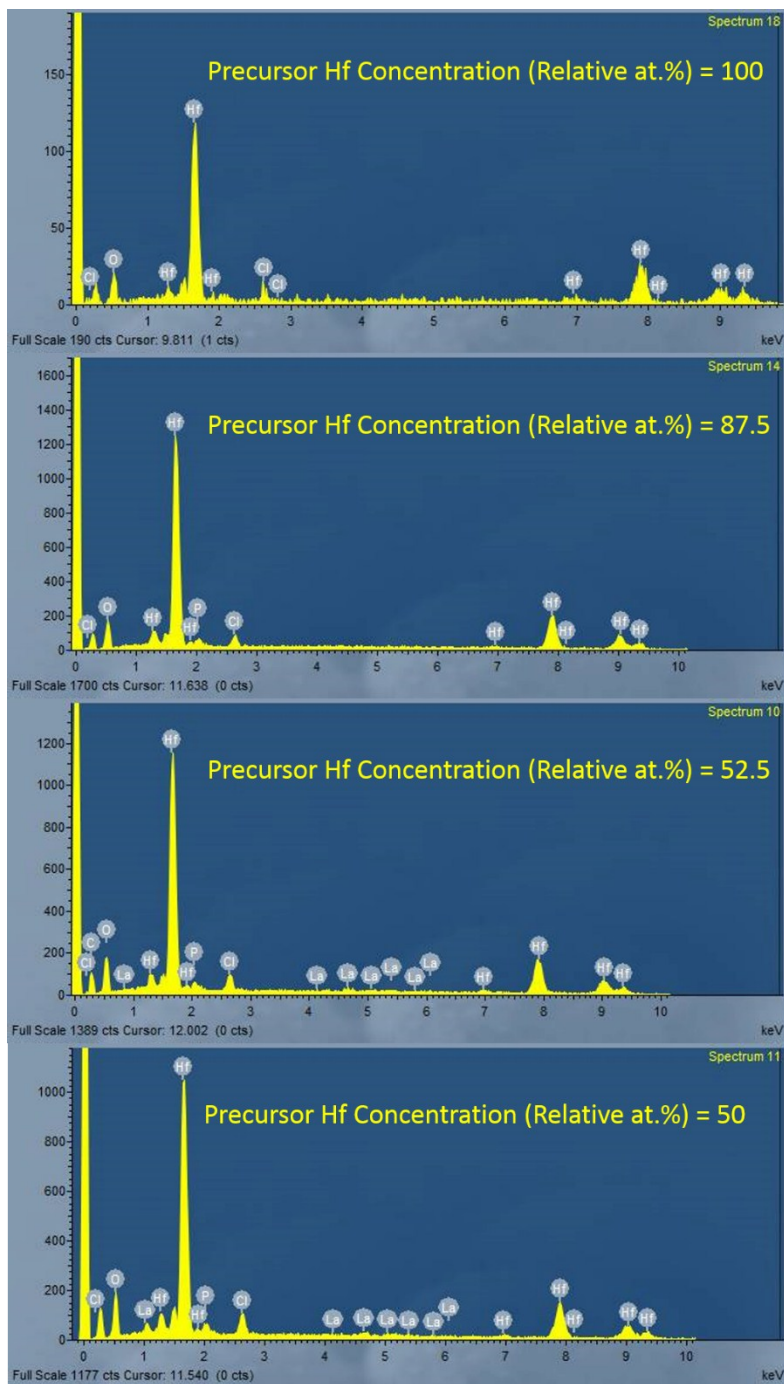


Figure S4. Energy dispersive X-ray spectroscopy (EDX) of pristine HfO_2 and selected $\text{Hf}_{1-x}\text{La}_x\text{O}_2$ nanocrystals. The detected concentrations of hafnium and lanthanum are listed in Table S3.

| Precursor Hf Concentration (Relative at.%) | Detected Hf Concentration by EDX (Relative at. %) | Detected La Concentration by EDX (Relative at. %) |
|--|---|---|
| 100 | 100 | 0 |
| 87.5 | 100 | Not Detected |
| 52.5 | 96.81 | 3.19 |
| 50 | 95.99 | 4.01 |

Table S3. Detected concentrations of hafnium and lanthanum by EDX analysis integrated from the spectra depicted in Figure S4.

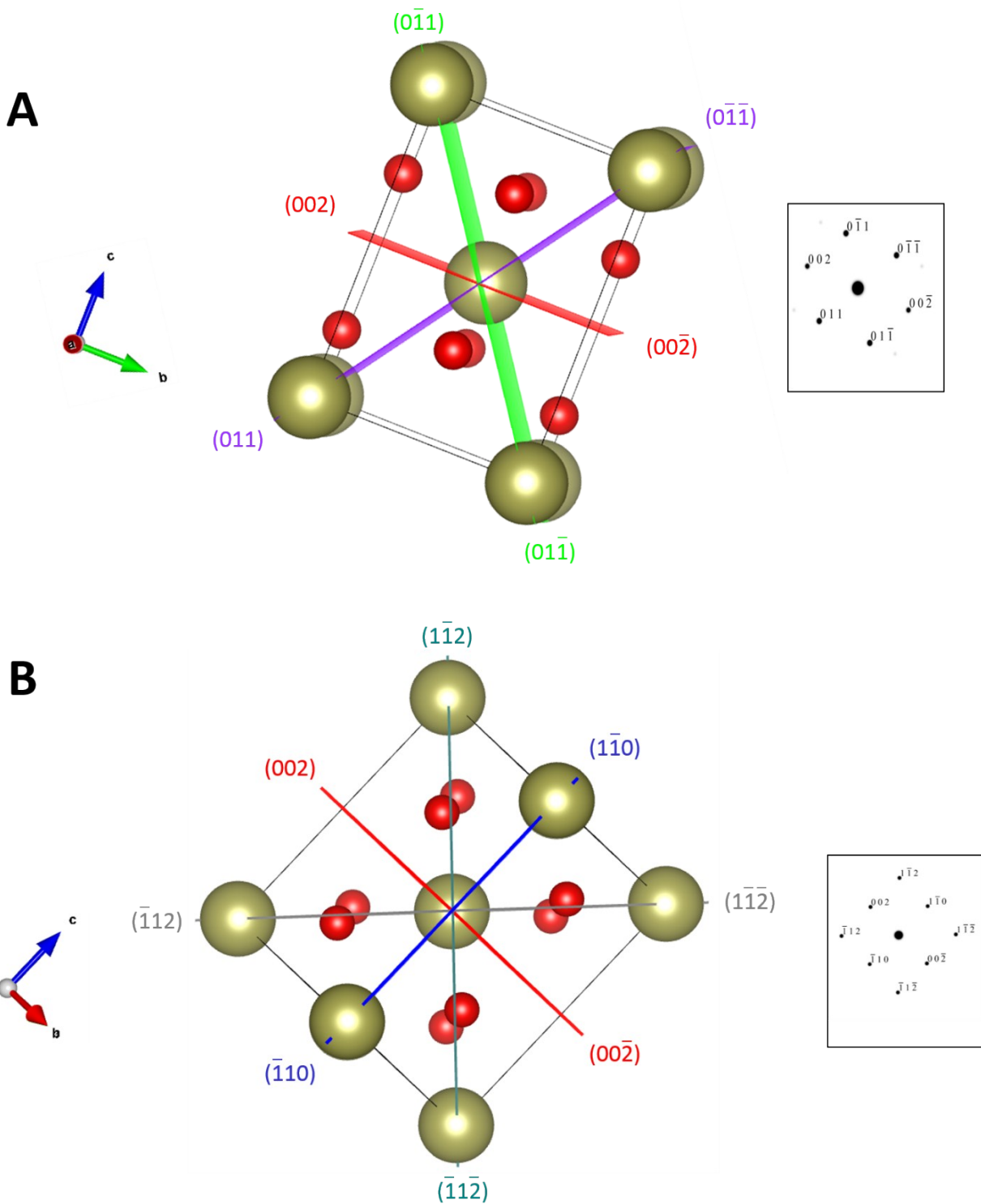


Figure S5. (A) HfO₂ tetragonal unit cell depicting the corresponding lattice planes from Figure 6D. (B) HfO₂ tetragonal unit cell depicting the corresponding lattice planes from Figure 6H. The unit cells are constructed using lattice parameters given in Ref. 40.